Approximate solution to the bidomain equations for electrocardiogram problems

Salil G. Patel and Bradley J. Roth
Department of Physics, Oakland University, Rochester, Michigan 48309, USA
(Received 8 August 2005; published 30 November 2005)

Simulating the electrocardiogram requires specifying the transmembrane potential distribution within the heart and calculating the potential on the surface of the body. Often, such calculations are based on the bidomain model of cardiac tissue. A subtle but fundamental problem arises when considering the boundary between the cardiac tissue and the surrounding volume conductor. In general, one finds that two potentials—the extracellular potential in the tissue and the potential in the surrounding bath—obey three boundary conditions, implying that the potentials are overdetermined. In this paper, we derive a general method for handling bidomain boundary conditions that eliminates this problem. The gist of the method is that we add an additional term to the transmembrane potential that falls exponentially with depth into the tissue. The purpose of this term is to satisfy the third boundary condition. Then, we take the limit as the length constant associated with this extra term goes to zero. Our result is two boundary conditions that approximately account for the full set of three boundary conditions at the tissue surface.

DOI: 10.1103/PhysRevE.72.051931 PACS number(s): 87.19.Hh, 87.10.+e

I. INTRODUCTION

An important topic in bioelectric theory is the calculation of the electrocardiogram (ECG) [1]. Often, such calculations are based on the bidomain model [2], a continuum model for the electrical properties of cardiac tissue that accounts for the anisotropy of both the intracellular space (inside the cardiac cells) and extracellular space (in the interstitial space between the cardiac cells). One way to approach this calculation is to specify the transmembrane potential distribution (the voltage across the cell membrane) within the heart and calculate the potential on the surface of the body. A subtle but fundamental problem arises in this calculation when considering the boundary between cardiac tissue and the surrounding volume conductor. In general, two potentials—the extracellular potential in the tissue and the potential in the surrounding bath—must obey three boundary conditions, implying that the potentials are overdetermined. In this paper, we derive an approximate method for handling the bidomain boundary conditions that eliminates this problem. We then compare our results to several previous calculations that used the bidomain model [3–8]. Our methods and results are analogous to a similar calculation we performed recently when studying defibrillation [9].

II. THE GENERAL PROBLEM

The bidomain equations governing the intracellular and extracellular potentials, V_i and V_e, are

$$\nabla \cdot (\tilde{g}_i \nabla V_i) = I_m, \tag{1}$$

$$\nabla \cdot (\tilde{g}_e \nabla V_e) = -I_m, \tag{2}$$

where $\tilde{g}_i$ and $\tilde{g}_e$ are the intracellular (i) and extracellular (e) conductivity tensors, and I_m is the membrane current. The quantities $\tilde{g}_i$ and $\tilde{g}_e$ are tensors because the electrical properties of cardiac tissue are anisotropic: they are different in the direction parallel to the fibers (longitudinal, L) than in the direction perpendicular to them (transverse, T). So four parameters describe the electrical properties of the tissue: the intracellular and extracellular conductivities in the longitudinal and transverse directions: g_{iL}, g_{iT}, g_{eL}, and g_{eT}. If the fiber direction changes throughout the tissue, the conductivity tensors also depend on the local fiber direction.

The bidomain equations are coupled, making them difficult to solve. Our goal is to uncouple them. Start with a change of variables

$$V_m = V_i - V_e, \quad \Psi = \frac{\alpha}{1+\alpha}\left(V_i + \frac{1}{\alpha} V_e\right), \tag{3}$$

with the inverse transformation

$$V_i = \Psi + \frac{1}{1+\alpha} V_m, \quad V_e = \Psi - \frac{\alpha}{1+\alpha} V_m, \tag{4}$$

where V_m is the transmembrane potential, Ψ is an auxiliary potential, and α is as yet unspecified. (The definition of Ψ is slightly different than in [10,11], but is the same as in [9].) If we write the bidomain equations in terms of these new potentials and then add Eqs. (1) and (2), we find

$$\nabla \cdot (\tilde{g}_i + \tilde{g}_e) \nabla \Psi = -\frac{1}{1+\alpha} \nabla \cdot (\tilde{g}_i - \alpha \tilde{g}_e) \nabla V_m. \tag{5}$$

In order to completely describe the bidomain problem, we need to account for the surrounding bath, of conductivity g_b, and the tissue-bath boundary conditions. Assume that the bath potential, V_b, obeys Laplace's equation,

$$\nabla^2 V_b = 0. \tag{6}$$

(A minor generalization would allow us to describe an anisotropic, inhomogeneous bath, but we will not consider that case in this study.) At the tissue-bath boundary, the boundary conditions are (i) the extracellular potential is equal to the bath potential, (ii) the normal component of the extracellular current density is equal to the normal component of the bath current density, and (iii) the normal component of the intra-

 ©2005 The American Physical Society

cellular current density is zero [12,13]. In almost all cases of interest, the cardiac fibers at the tissue surface lie parallel to the surface. We will assume that this is the case throughout the rest of the analysis. Mathematically, we can write the boundary conditions as

$$V_e = V_b, \tag{7}$$

$$g_{eT}\frac{\partial V_e}{\partial n} = g_b\frac{\partial V_b}{\partial n}, \tag{8}$$

$$g_{iT}\frac{\partial V_i}{\partial n} = 0, \tag{9}$$

where n is the direction perpendicular to the surface, going into the tissue. Now we need to express these boundary conditions in terms of the variables V_m and Ψ. If we use Eq. (4) and some algebra, the boundary conditions become

$$\Psi - \frac{\alpha}{1+\alpha}V_m = V_b, \tag{10}$$

$$g_{eT}(1+\alpha)\frac{\partial \Psi}{\partial n} = g_b\frac{\partial V_b}{\partial n}, \tag{11}$$

$$\frac{\partial V_m}{\partial n} = -(1+\alpha)\frac{\partial \Psi}{\partial n}. \tag{12}$$

Finally, the outer edge of the bath has boundary conditions. For instance, V_b may be specified on the boundary, the boundary may be sealed ($\partial V_b/\partial n = 0$), or V_b may go to zero far from the heart. The choice of boundary conditions depends on the physical situation.

When calculating the ECG, V_m is the known source term, and the goal is to calculate V_e (or, in our analysis, Ψ) and V_b. In this case, Eqs. (5) and (6) govern Ψ and V_b, and Eqs. (10)–(12) are the boundary conditions. Unfortunately, there is a problem with this approach, and it is fundamental. The three boundary conditions at the tissue-bath surface overdetermine Ψ and V_b. That is, V_m cannot be chosen arbitrarily if we wish to fulfill all three boundary conditions. For example, if V_m is taken as independent of depth into the tissue (independent of n), then the normal derivative of V_m in Eq. (12) is zero, implying that the normal derivative of Ψ is also zero, which by Eq. (11) implies that the normal derivative of V_b is zero. This means that no current passes from the tissue to the bath, which does not make physical sense, and we conclude that such a specification of V_m is not consistent with the bidomain equations. To make further progress, we must overcome this problem.

To keep the analysis simple, assume that the fibers lie along the direction of one of the coordinate axes; for instance, in the x direction in Cartesian coordinates, or in the θ direction in spherical coordinates. Furthermore, assume that V_m corresponds to a wave front propagating either parallel to or perpendicular to the fibers. Let α be the ratio of intracellular to extracellular conductivities in the direction of propagation. For instance, if propagation is along the fibers, $\alpha = g_{iL}/g_{eL}$. This definition of α ensures that the factor $\tilde{g}_i - \alpha\tilde{g}_e$ on the right side of Eq. (5) is zero in the direction of propagation. If we were considering a planar wave front, in the sense that it propagates along the fibers but is uniform in the direction perpendicular to the fibers, then the gradient of V_m in the direction perpendicular to the fibers would be zero. Therefore the entire right-hand side of Eq. (5) would vanish, and Ψ would obey

$$\nabla \cdot (\tilde{g}_i + \tilde{g}_e)\nabla \Psi = 0. \tag{13}$$

However, the planar wave front assumption violates the boundary conditions, as described earlier. It cannot be correct. We need to modify V_m so it has some variation perpendicular to the direction of the fibers (and therefore perpendicular to the surface).

Let V_m be given by

$$V_m = V + Ae^{-n/\lambda}, \tag{14}$$

where V represents a planar wave front (no variation perpendicular to the surface). V acts as our source term, which we can specify as we wish. $Ae^{-n/\lambda}$ is an additional term whose sole purpose is to ensure the boundary conditions are not violated [9]. We can think of λ as being related to the electrical length constant in the direction perpendicular to the fibers, but for our purposes it need not be identical to this length constant. A can vary in the plane of the surface, but is not a function of depth.

The expression for V_m in Eq. (14) will contribute to the right-hand side of Eq. (5). Recall that the right-hand side is zero in the direction parallel to the fibers because of the definition of α. However, the additional term contributes to the right-hand side in the direction perpendicular to the fibers. In order to make the left-hand side of Eq. (5) equal to the right-hand side, Ψ must have a similar additional term. Specifically, we write Ψ as the sum of Ψ_0, the solution to the homogeneous equation [Eq. (13)], and an additional exponential term

$$\Psi = \Psi_0 + Be^{-n/\lambda}. \tag{15}$$

If we plug Eqs. (14) and (15) into Eq. (5) and only consider derivatives perpendicular to the tissue surface, we find that A and B are related by

$$B = -\frac{1}{1+\alpha}\frac{g_{iT} - \alpha g_{eT}}{g_{iT} + g_{eT}}A. \tag{16}$$

Finally, we can substitute Eqs. (14) and (15) into the boundary conditions in Eqs. (10)–(12) and simplify. We find

$$A = \frac{g_{iT} + g_{eT}}{g_{eT}}\lambda\frac{\partial \Psi_0}{\partial n}, \tag{17}$$

$$B = -\frac{g_{iT} - \alpha g_{eT}}{g_{eT}(1+\alpha)}\lambda\frac{\partial \Psi_0}{\partial n}, \tag{18}$$

and two boundary conditions for Ψ and V_b.

Now we make another assumption. Let the variation of the potentials in the plane of the surface be small compared to the variation in depth. In other words, assume λ is small compared to the distance over which Ψ and V_m vary in the plane of the surface. This assumption would not be valid if

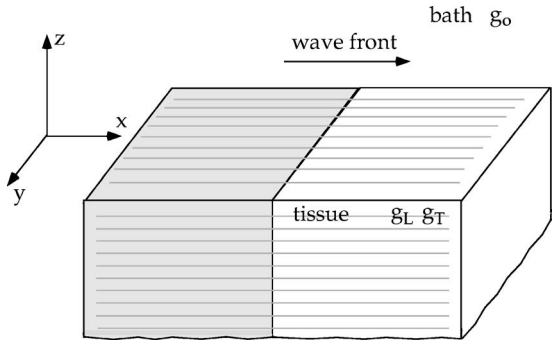

FIG. 1. A planar wave front propagating along a half-infinite block of cardiac tissue, perfused by a bath of conductivity g_o. The gray lines indicate the fiber direction. The shaded tissue represents the action potential.

we were concerned with local, high spatial frequency effects, such as changes in the rate of rise of V_m at the tissue surface [6]. However, when analyzing the ECG we are often concerned with only the low spatial frequencies that contribute to the bath potential far from the heart. In the limit as λ goes to zero, A and B vanish and the two boundary conditions become (for notational simplicity, we drop the subscript from Ψ and let $g_T = g_{iT} + g_{eT}$)

$$-\frac{\alpha}{1+\alpha}V + \Psi = V_b, \tag{19}$$

$$g_T \frac{\partial \Psi}{\partial n} = g_b \frac{\partial V_b}{\partial n}. \tag{20}$$

This completes our approximate formulation of the bidomain problem. Ψ is the solution to the homogeneous problem, Eq. (13), and V_b is the solution to Laplace's equation, Eq. (6). The boundary conditions are given by Eqs. (19) and (20). V is the planar wave front source term. The additional terms in Eqs. (14) and (15) allow us to enforce all the boundary conditions. Even though we ultimately take the limit as λ goes to zero, these extra terms still influence the solution. Now that we have this approximate formulation of the bidomain calculation, let us consider some simple examples.

III. EXAMPLE 1: TWO-DIMENSIONAL TISSUE ANALYSIS

As an example, consider a slab of tissue in the region $z < 0$, which is perfused by a bath ($z > 0$). Assume a planar wave front propagates in the x direction (parallel to the fibers), and let this wave front be independent of y (Fig. 1). This problem was first examined by Plonsey and Barr [4]. Equations (6) and (13) become

$$\frac{\partial^2 V_b}{\partial x^2} + \frac{\partial^2 V_b}{\partial z^2} = 0, \tag{21}$$

$$(g_{iL} + g_{eL})\frac{\partial^2 \Psi}{\partial x^2} + (g_{iT} + g_{eT})\frac{\partial^2 \Psi}{\partial z^2} = 0. \tag{22}$$

Let V vary sinusoidally in the x direction, with spatial frequency k. This is not really a restriction, since we can view this potential as one component of a Fourier expansion. The solutions to Eqs. (21) and (22) are

$$V_b(x,z) = Ce^{-kz}\sin kx, \tag{23}$$

$$\Psi(x,z) = De^{\sqrt{g_L/g_T}kz}\sin kx, \tag{24}$$

where $g_L = g_{iL} + g_{eL}$. If we substitute Eqs. (23) and (24) into the boundary conditions in Eqs. (19) and (20), we get

$$C = -\frac{\alpha}{1+\alpha}V\frac{1}{1+\frac{g_b}{\sqrt{g_T g_L}}}, \tag{25}$$

$$D = \frac{\alpha}{1+\alpha}V\frac{1}{1+\frac{\sqrt{g_T g_L}}{g_b}}. \tag{26}$$

If the bath conductivity goes to zero, C approaches $-[\alpha/(1+\alpha)]V$ and D goes to zero.

Johnston *et al.* [8] have solved a similar problem using different boundary conditions. Let us examine the difference between our method of determining C and D and theirs. Johnston *et al.* use two boundary conditions, one of which is Eq. (19) and the other one is equivalent to

$$g_{eT}\frac{\partial \Psi}{\partial n} = g_b \frac{\partial V_b}{\partial n}. \tag{27}$$

Moreover, they do not use the assumption given by Eq. (14), but instead assume V_m is independent of depth, $V_m(x) = V\sin kx$ (that is, $A = B = 0$). As we said earlier, this set of boundary conditions is not self-consistent, and it is instructive to examine what result their method gives. If we plug the expressions given in Eqs. (23) and (24) into Eqs. (19) and (27), and solve for C and D, we get

$$C = -\frac{\alpha}{1+\alpha}V\frac{1}{1+\frac{g_T}{g_{eT}}\frac{g_b}{\sqrt{g_T g_L}}}, \tag{28}$$

$$D = \frac{\alpha}{1+\alpha}V\frac{1}{1+\frac{g_{eT}}{g_T}\frac{\sqrt{g_T g_L}}{g_b}}. \tag{29}$$

The expression for C, which determines the bath potential, is different in Eqs. (25) and (28) by a factor of g_T/g_{eT} in the denominator. If we use the conductivity values consistent with those given in [14]—$g_{iL} = 0.2$ S/m, $g_{eL} = 0.2$ S/m, $g_{iT} = 0.02$ S/m, and $g_{eT} = 0.08$ S/m—and a bath conductivity of $g_b = 1$ S/m, we find that Johnston *et al.*'s value of C is about 17% smaller than ours. This difference may be significant in precise quantitative measurements, but is probably not important for qualitative analysis, of the ECG.

IV. EXAMPLE 2: PLANAR SLAB MODEL

In a minor generalization of the previous model, Henriquez *et al.* [5] examined a slab of cardiac tissue of thick-

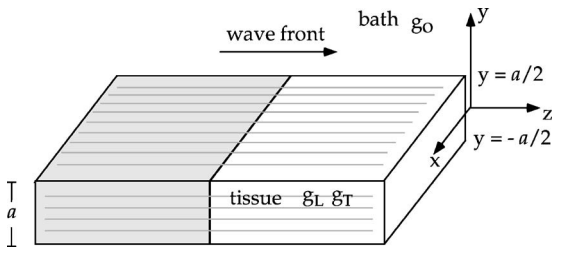

FIG. 2. A planar wave front propagating along a slab of cardiac tissue, of thickness a, perfused on both sides ($y > a/2$, $y < -a/2$) by a bath of conductivity g_o. The gray lines indicate the fiber direction. The shaded tissue represents the action potential.

ness $2a$, with an action potential propagating in the z direction, independent of x, with y being the direction perpendicular to the tissue surface (the coordinate directions are labeled slightly differently here than in the previous example, to stay consistent with [5]) (Fig. 2). The relationships among $V_b(y,z)$, $\Psi(y,z)$, and $V_m(z)$ are most conveniently expressed in terms of Fourier transforms. For example, the Fourier transform of the potential $V(z)$, designated $\hat{V}(k)$, is defined by

$$\hat{V}(k) = \int_{-\infty}^{\infty} V(z) e^{+ikz} dz, \tag{30}$$

with the inverse relation being

$$V(z) = \frac{1}{2\pi} \int_{-\infty}^{\infty} \hat{V}(k) e^{-ikz} dk. \tag{31}$$

The variable k represents a spatial frequency.

We can solve Eqs. (6) and (13) with boundary conditions (19) and (20), and find that $\hat{\Psi}(y,k)$ and $\hat{V}_b(y,k)$, the Fourier transforms of $\Psi(y,z)$ and $V_b(y,z)$, can be written in terms of $\hat{V}(k)$ as

$$\hat{\Psi}(\rho,k) = \frac{\alpha}{1+\alpha} \frac{\cosh(k\delta y)}{\cosh(k\delta a)\beta(|k|,a,\delta)} \hat{V}(k), \tag{32}$$

$$\hat{V}_b(\rho,k) = \frac{\alpha}{1+\alpha} \frac{e^{-ky}}{e^{-ka}\alpha(|k|,a,\delta)} \hat{V}(k), \tag{33}$$

where the functions $\alpha(|k|,a,\delta)$, $\beta(|k|,a,\delta)$, and $\gamma(|k|,a,\delta)$ are defined as

$$\alpha(|k|,a,\delta) = -[1+\gamma(|k|,a,\delta)], \tag{34}$$

$$\beta(|k|,a,\delta) = 1 + \frac{1}{\gamma(|k|,a,\delta)}, \tag{35}$$

$$\gamma(|k|,a,\delta) = \frac{g_b}{\sqrt{g_L g_T}} \frac{1}{\tanh(k\delta a)}, \tag{36}$$

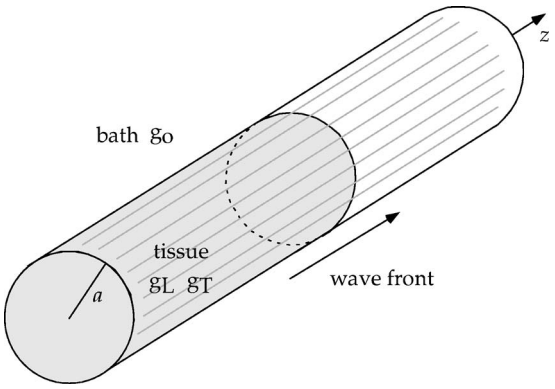

FIG. 3. A planar wave front propagating along a cylinder of cardiac tissue, of radius a, perfused by a bath of conductivity g_o. The gray lines indicate the fiber direction. The shaded tissue represents the action potential.

and $\delta = \sqrt{g_L/g_T}$. These results are equivalent to those derived by Henriquez *et al.* [5], who assumed equal anisotropy ratios in their derivation. They are not, however, equivalent to the results obtained if one assumes that the intracellular, rather than the transmembrane, potential is independent of depth [6].

V. EXAMPLE 3: A CYLINDRICAL FIBER

One limitation of the two previous examples was that the tissue was unbounded in the direction perpendicular to propagation. In that case, we cannot examine how the potential depends on the cross-sectional area of the wave front, because it is infinite. We can remove this limitation by considering propagation along a cylindrical fiber (Fig. 3). We represent the tissue as a cylinder of radius a and describe it with cylindrical coordinates (ρ, θ, z). The fibers lie along the z axis, and the cylindrical symmetry ensures that the potential is independent of the angle θ. Again, the relationships among $V_b(\rho,z)$, $\Psi(\rho,z)$, and $V(z)$ are expressed in terms of Fourier transforms.

We can solve Eqs. (6) and (13) with boundary conditions (19) and (20), and find that $\hat{\Psi}(\rho,k)$ and $\hat{V}_b(\rho,k)$, the Fourier transforms of $\Psi(\rho,z)$ and $V_b(\rho,z)$, can be written in terms of $\hat{V}(k)$ as

$$\hat{\Psi}(\rho,k) = \frac{\alpha}{1+\alpha} \frac{I_0(|k|\delta\rho)}{I_0(|k|\delta a)\beta(|k|,a,\delta)} \hat{V}(k), \tag{37}$$

$$\hat{V}_b(\rho,k) = \frac{\alpha}{1+\alpha} \frac{K_0(|k|\rho)}{K_0(|k|a)\alpha(|k|,a,\delta)} \hat{V}(k), \tag{38}$$

where the functions $\alpha(|k|,a,\delta)$, $\beta(|k|,a,\delta)$, and $\gamma(|k|,a,\delta)$ are defined as

$$\alpha(|k|,a,\delta) = -[1+\gamma(|k|,a,\delta)] \tag{39}$$

$$\beta(|k|,a,\delta) = 1 + \frac{1}{\gamma(|k|,a,\delta)} \tag{40}$$

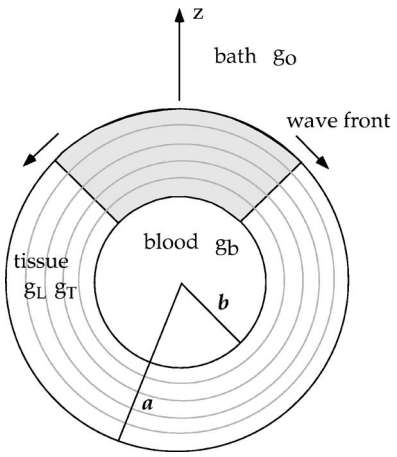

FIG. 4. A planar wave front propagating through a spherical shell of cardiac tissue of inner radius b and outer radius a. The shell is surrounded by a bath of conductivity g_o, and encloses blood of conductivity g_b. The gray circles indicate the fiber direction. The shaded tissue represents the action potential.

$$\gamma(|k|,a,\delta) = \frac{g_b I_0(|k|\delta a) K_1(|k|a)}{\sqrt{g_L g_T} I_1(|k|\delta a) K_0(|k|a)}, \tag{41}$$

and $\delta = \sqrt{g_L/g_T}$. These results are equivalent to those derived by Roth and Wikswo [3], who assumed V_m was independent of depth, did not enforce the boundary condition in Eq. (9), and replaced the boundary condition in Eq. (8) with

$$g_{iT}\frac{\partial V_i}{\partial n} + g_{eT}\frac{\partial V_e}{\partial n} = g_b \frac{\partial V_b}{\partial n}. \tag{42}$$

VI. EXAMPLE 4: THE SPHERICAL HEART

Li *et al.* [7] represented the heart as a spherical shell of cardiac tissue. Their model consists of cardiac tissue surrounding a blood cavity and surrounded by a conducting bath (Fig. 4). The inner and outer radii of the shell are b and a, and the conductivity of the blood and bath are g_b and g_o. The fibers are in the θ direction, and azimuthal symmetry implies that the potential is independent of the angle ϕ. In spherical coordinates (r,θ,ϕ), Eq. (13) for Ψ is

$$g_T \frac{1}{r}\frac{\partial^2}{\partial r^2}(r\Psi) + g_L \frac{1}{r^2}\frac{1}{\sin\theta}\frac{\partial}{\partial\theta}\left(\sin\theta\frac{\partial\Psi}{\partial\theta}\right) = 0, \tag{43}$$

and V_o and V_b obey Laplace's equation. We assume that the source term in the transmembrane potential depends only on θ, and write it as an expansion in Legendre polynomials

$$V(\theta) = \sum_{l=0}^{\infty} V_l P_l(\cos\theta). \tag{44}$$

If $V(\theta)$ has the form $V(\theta)=V_o$ for $\theta<\theta_o$ and $V(\theta)=0$ for $\theta>\theta_o$, then $V_0 = V_o(\cos\theta_o - 1)/2$ and $V_l = V_o[P_{l+1}(\cos\theta_o) - P_{l-1}(\cos\theta_o)]/2$ for $l \geqslant 1$ [7]. In particular, the $l=1$ term reduces to $V_1 = (3/4)\sin^2\theta_o$.

The general solutions for the potentials are [15]

$$\Psi = \sum_{l=0}^{\infty} (C_l r^{\nu_1} + D_l r^{\nu_2}) P_l(\cos\theta), \tag{45}$$

$$V_b = \sum_{l=0}^{\infty} B_l r^l P_l(\cos\theta), \tag{46}$$

$$V_o = \sum_{l=0}^{\infty} \frac{A_l}{r^{l+1}} P_l(\cos\theta), \tag{47}$$

where

$$\nu_{1,2} = -\frac{1}{2} \pm \sqrt{l(l+1)\frac{g_L}{g_T} + \frac{1}{4}}. \tag{48}$$

We determine constants A_l, B_l, C_l, and D_l by applying the boundary conditions $-[\alpha/(1+\alpha)]V + \Psi = V_b$ and $g_T(\partial\Psi/\partial r) = g_b(\partial V_b/\partial r)$ at $r=b$ and $-[\alpha/(1+\alpha)]V + \Psi = V_o$ and $g_T(\partial\Psi/\partial r) = g_o(\partial V_o/\partial r)$ at $r=a$, and obtain

$$A_l = -\frac{\left(\frac{a}{b}\right)^{\nu_1+\nu_2}(\nu_2-\nu_1) + \nu_1\left(\frac{a}{b}\right)^{\nu_1} - \nu_2\left(\frac{a}{b}\right)^{\nu_2} + \frac{g_T\nu_1\nu_2}{g_b l}\left[\left(\frac{a}{b}\right)^{\nu_2} - \left(\frac{a}{b}\right)^{\nu_1}\right]}{\left(\frac{a}{b}\right)^{\nu_1}\left(1 - \frac{g_T}{g_b}\frac{\nu_2}{l}\right)\left(1 + \frac{g_T}{g_o}\frac{\nu_1}{l+1}\right) - \left(\frac{a}{b}\right)^{\nu_2}\left(1 - \frac{g_T}{g_b}\frac{\nu_1}{l}\right)\left(1 + \frac{g_T}{g_o}\frac{\nu_2}{l+1}\right)} \frac{g_T}{g_o(l+1)} a^{l+1}\frac{\alpha}{1+\alpha}V_l, \tag{49}$$

$$B_l = \frac{\nu_1 - \nu_2 - \nu_1\left(\frac{a}{b}\right)^{\nu_2} + \nu_2\left(\frac{a}{b}\right)^{\nu_1} + \frac{g_T\nu_1\nu_2}{g_o(l+1)}\left[\left(\frac{a}{b}\right)^{\nu_1} - \left(\frac{a}{b}\right)^{\nu_2}\right]}{\left(\frac{a}{b}\right)^{\nu_1}\left(1 - \frac{g_T}{g_b}\frac{\nu_2}{l}\right)\left(1 + \frac{g_T}{g_o}\frac{\nu_1}{l+1}\right) - \left(\frac{a}{b}\right)^{\nu_2}\left(1 - \frac{g_T}{g_b}\frac{\nu_1}{l}\right)\left(1 + \frac{g_T}{g_o}\frac{\nu_2}{l+1}\right)} \frac{g_T}{g_b l}\frac{1}{b^l}\frac{\alpha}{1+\alpha}V_l, \tag{50}$$

$$C_l = \frac{\left(1 - \frac{g_T}{g_b}\frac{\nu_2}{l}\right) - \left(\frac{a}{b}\right)^{\nu_2}\left(1 + \frac{g_T}{g_o}\frac{\nu_2}{l+1}\right)}{\left(\frac{a}{b}\right)^{\nu_1}\left(1 - \frac{g_T}{g_b}\frac{\nu_2}{l}\right)\left(1 + \frac{g_T}{g_o}\frac{\nu_1}{l+1}\right) - \left(\frac{a}{b}\right)^{\nu_2}\left(1 - \frac{g_T}{g_b}\frac{\nu_1}{l}\right)\left(1 + \frac{g_T}{g_o}\frac{\nu_2}{l+1}\right)} \frac{1}{b^{\nu_1}} \frac{\alpha}{1+\alpha} V_l, \tag{51}$$

$$D_l = \frac{\left(\frac{a}{b}\right)^{\nu_1}\left(1 + \frac{g_T}{g_o}\frac{\nu_1}{l+1}\right) - \left(1 - \frac{g_T}{g_b}\frac{\nu_1}{l}\right)}{\left(\frac{a}{b}\right)^{\nu_1}\left(1 - \frac{g_T}{g_b}\frac{\nu_2}{l}\right)\left(1 + \frac{g_T}{g_o}\frac{\nu_1}{l+1}\right) - \left(\frac{a}{b}\right)^{\nu_2}\left(1 - \frac{g_T}{g_b}\frac{\nu_1}{l}\right)\left(1 + \frac{g_T}{g_o}\frac{\nu_2}{l+1}\right)} \frac{1}{b^{\nu_2}} \frac{\alpha}{1+\alpha} V_l. \tag{52}$$

For the ECG problem, we are most concerned about A_l for small values of l. For $l=0$, $A_l=0$, so there is no monopole contribution to the bath potential. For $l=1$, the bath potential has the form of a dipole

$$V_o(r,\theta) = \frac{p\cos\theta}{4\pi g_o r^2}, \tag{53}$$

where the dipole moment p is given by

$$p = \frac{3}{2}\pi a^2 g_T V_o \sin^2\theta_o \frac{\alpha}{1+\alpha}\left\{\frac{-\left(\frac{a}{b}\right)^{\nu_1+\nu_2}(\nu_2-\nu_1) - \nu_1\left(\frac{a}{b}\right)^{\nu_1} + \nu_2\left(\frac{a}{b}\right)^{\nu_2} - \frac{g_T\nu_1\nu_2}{g_b}\left[\left(\frac{a}{b}\right)^{\nu_2} - \left(\frac{a}{b}\right)^{\nu_1}\right]}{\left(\frac{a}{b}\right)^{\nu_1}\left(1 - \frac{g_T}{g_b}\nu_2\right)\left(1 + \frac{g_T}{g_o}\frac{\nu_1}{2}\right) - \left(\frac{a}{b}\right)^{\nu_2}\left(1 - \frac{g_T}{g_b}\nu_1\right)\left(1 + \frac{g_T}{g_o}\frac{\nu_2}{2}\right)}\right\}. \tag{54}$$

This result indicates how the bath potential depends on parameters such as a, b, g_o, and g_b. It is a generalization of the Li *et al.* [7] result because it allows the tissue to be anisotropic, and it is not limited to the case when $g_o=0$.

VII. DISCUSSION

The ECG forward problem can be formulated as shown in Fig. 5: Eqs. (6) and (13), with boundary conditions in Eqs. (19) and (20). This formulation ensures that all three boundary conditions [Eqs. (7)–(9)] are satisfied. It is an approximate method and is based on the assumption that additional terms added to V_m and Ψ have an exponential form, and their length constant is small compared to other distances. In some cases, our formulation gives results that are consistent with those obtained previously [3,5], and in other cases the results are different [6–8]. Our results are similar to those we found previously when considering electrical stimulation and defibrillation [9].

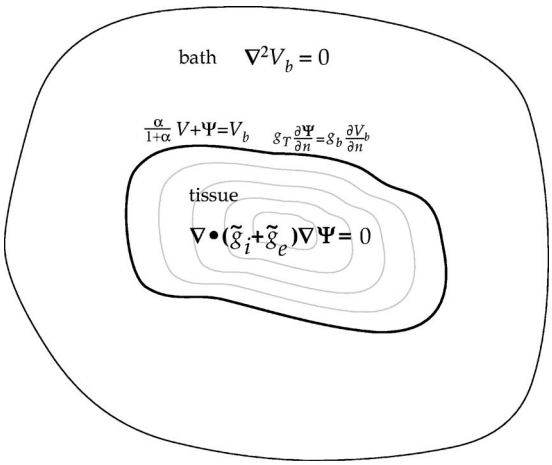

FIG. 5. A schematic diagram of the boundary value problem for Ψ and V_b. The function V is the known transmembrane potential source term. The gray curves indicate the fiber direction. If V depends on the direction perpendicular to the fibers, then the equation for Ψ in the tissue should be replaced by Eq. (5).

We analyzed the case when the tissue surrounding the heart is isotropic, homogeneous, and unbounded, but extending the analysis to remove this limitation would be straightforward. Also, we considered only planar wave fronts propagating parallel to the fiber direction, and simple fiber geometries. We can generalize the method to arbitrary wave fronts and fiber geometries if we replace Eq. (13) for Ψ by Eq. (5). Our analysis of the proper boundary conditions at the heart surface should be valuable as researchers use the bidomain model to study more realistic heart and torso geometries [16,17], and phenomena such as ST segment shift during ischemia [18–20].

ACKNOWLEDGMENTS

This work was supported by grants from the National Institutes of Health (RO1 HL57207) and the American Heart Association—Midwest Affiliate.

[1] R. M. Gulrajani, Crit. Rev. Biomed. Eng. **16**, 1 (1988).
[2] C. S. Henriquez, Crit. Rev. Biomed. Eng. **21**, 1 (1993).
[3] B. J. Roth and J. P. Wikswo, Jr., IEEE Trans. Biomed. Eng. **33**, 467 (1986).
[4] R. Plonsey and R. C. Barr, Biophys. J. **51**, 547 (1987).
[5] C. S. Henriquez, N. Trayanova, and R. Plonsey, Ann. Biomed. Eng. **18**, 367 (1990).
[6] B. J. Roth, Ann. Biomed. Eng. **24**, 639 (1996).
[7] D. Li, C. Y. Li, A. C. Yong, P. R. Johnston, and D. Kilpatrick, Circ. Res. **85**, 959 (1999).
[8] P. R. Johnston, D. Kilpatrick, and C. Y. Li, IEEE Trans. Biomed. Eng. **48**, 1366 (2001).
[9] S. G. Patel and B. J. Roth, Phys. Rev. E **71**, 021908 (2005).
[10] B. J. Roth, Phys. Rev. E **55**, 1819 (1997).
[11] B. J. Roth and D. Langrill Beaudoin, Phys. Rev. E **67**, 051925 (2003).
[12] B. J. Roth, Ann. Biomed. Eng. **19**, 669 (1991).
[13] W. Krassowska and J. C. Neu, IEEE Trans. Biomed. Eng. **41**, 143 (1994).
[14] B. J. Roth, IEEE Trans. Biomed. Eng. **44**, 326 (1997).
[15] N. A. Trayanova, B. J. Roth, and L. J. Malden, IEEE Trans. Biomed. Eng. **40**, 899 (1993).
[16] B. Hopenfeld, J. G. Stinstra, and R. S. MacLeod, J. Cardiovasc. Electrophysiol. **15**, 1200 (2004).
[17] M. C. MacLachlan, J. Sundnes, and G. L. Lines, IEEE Trans. Biomed. Eng. **52**, 799 (2005).
[18] D. Kilpatrick, P. R. Johnston, and D. S. Li, J. Electrocardiol. **36** (Suppl.), 7 (2003).
[19] P. R. Johnston and D. Kilpatrick, IEEE Trans. Biomed. Eng. **50**, 150 (2003).
[20] P. R. Johnston, Math. Biosci. **186**, 43 (2003).